Journal of Neurochemistry

JOURNAL OF NEUROCHEMISTRY | 2009 | 111 | 1213–1224 doi: 10.1111/j.1471-4159.2009.06399.x

Suppression of APP-containing vesicle trafficking and production of β-amyloid by AID/DHHC-12 protein

Chie Mizumaru, Yuhki Saito, Takao Ishikawa, Tomohiro Yoshida, Tohru Yamamoto, Tadashi Nakaya and Toshiharu Suzuki

Laboratory of Neuroscience, Graduate School of Pharmaceutical Sciences, Hokkaido University, Sapporo, Japan

Abstract

The metabolism of amyloid β-protein precursor (APP) is regulated by various cytoplasmic and/or membrane-associated proteins, some of which are involved in the regulation of intracellular membrane trafficking. We found that a protein containing Asp–His–His–Cys (DHHC) domain, alcadein and APP interacting DHHC protein (AID)/DHHC-12, strongly inhibited APP metabolism, including amyloid β-protein (Aβ) generation. In cells expressing AID/DHHC-12, APP was tethered in the Golgi, and APP-containing vesicles disappeared from the cytoplasm. Although DHHC domain-containing proteins are involved in protein palmitoylation, a AID/DHHC-12 mutant of which the enzyme activity was impaired by replacing the DHHC sequence with Ala–Ala–His–Ser (AAHS) made no detectable difference in the generation and trafficking of APP-containing vesicles in the cytoplasm or the metabolism of APP. Furthermore, the mutant AID/DHHC-12 significantly increased non-amyloidogenic α-cleavage of APP along with activation of a disintegrin and metalloproteinase 17, a major α-secretase, suggesting that protein palmitoylation involved in the regulation of α-secretase activity. AID/DHHC-12 can modify APP metabolism, including Aβ generation in multiple ways by regulating the generation and/or trafficking of APP-containing vesicles from the Golgi and their entry into the late secretary pathway in an enzymatic activity-independent manner, and the α-cleavage of APP in the enzymatic activity-dependent manner.

Keywords: amyloid β-protein precursor, amyloid β-protein, DHHC protein, Golgi, α-secretase, membrane trafficking.

J. Neurochem. (2009) **111**, 1213–1224.

Alzheimer's disease (AD) is a common progressive neurodegenerative disease characterized pathologically by appearance of senile plaques and neurofibrillary tangles in the patient's brain. The major protein component of senile plaques is amyloid β-protein (Aβ). It is believed that Aβ aggregates and/or forms oligomers prior to formation of neurofibrillary tangles in the brain and that these Aβ clusters have a seminal role in AD pathogenesis. The Aβ is generated from amyloid β-protein precursor (APP), a type I transmembrane protein, by consecutive cleavages by the β-site APP-cleaving enzyme (BACE) and γ-secretase complex (reviewed in Selkoe 2001; Gandy 2005). Recent analyzes suggested that APP is subject to cleavage in the secretary pathways interconnecting the Golgi apparatus, plasma membrane, and endosomes (reviewed in Small and Gandy 2006; Thinakaran and Koo 2008). Therefore, understanding how the intracellular trafficking of APP is regulated together with membrane-associated APP-metabolic enzymes, such as BACE, α-site-cleaving enzyme/α-secretase, and γ-secretase, including presenilin, is important to understand the pathogenesis of AD (reviewed in Suzuki *et al.* 2006).

Several proteins interact with the cytoplasmic region of APP to regulate APP trafficking (reviewed in Suzuki and Nakaya 2008). For example, C-Jun NH2-terminal kinase

Received April 9, 2009; revised manuscript received September 9, 2009; accepted September 16, 2009.

Address correspondence and reprint requests to Toshiharu Suzuki, Laboratory of Neuroscience, Graduate School of Pharmaceutical Sciences, Hokkaido University, Kita12-Nishi6, Kita-ku, Sapporo 060-0812, Japan. E-mail: tsuzuki@pharm.hokudai.ac.jp

Abbreviations used: Aβ, amyloid β-protein; AAHS, Ala–Ala–His–Ser; AD, Alzheimer's disease; ADAM, a disintegrin and metalloproteinase; ADAM17-HA, HA-tagged ADAM17; AID, alcadein and APP interacting DHHC protein; Alc, Alcadein; APP, amyloid β-protein precursor; APP-CTF, the carboxyl-terminal fragment of APP cleaved at α- or β- site; BACE, β-site APP-cleaving enzyme; DHHC, Asp–His–His–Cys; EGFP, enhanced GFP; FLAG, a protein composed of N-DYKDDDDK-C; GFP, green fluorescence protein; GST, glutathione-S-transferase; HA, hemaglutinin; imAPP, immature APP; JNK, C-jun-NH2-terminal kinase; mAPP, mature APP; mRFP, monomeric red fluorescence protein; N2a, mouse neuroblastoma Neuro 2a; PBST, phosphate-buffered saline containing 0.05% (v/v) Tween 20; sAPP, secreted large amino-terminal fragments of APP; SDS, sodium dodecyl sulfate; TGN, *trans*-Golgi network.

(JNK)-interacting protein 1b associates with the cytoplasmic region of APP to load APP onto the kinein-1 motor for the anterograde transport of APP-containing vesicles (Gunawardena and Goldstein 2001; Matsuda *et al.* 2001; Taru *et al.* 2002; Inomata *et al.* 2003; Araki *et al.* 2007). APP also interacts with the retromer, which transports APP to the endosome from the cell surface (Anderson *et al.* 2005; Offe *et al.* 2006). Furthermore, presenilin is also thought to be involved in a membrane protein trafficking (Naruse *et al.* 1998; Wang *et al.* 2004). However, it is still unclear how APP-containing vesicles are generated from the Golgi, where is the point of origin for vesicular trafficking of APP to the distal regions within a cell.

Here, we found that the largely Golgi-localized protein alcadein and APP interacting DHHC protein (AID)/Asp–His–His–Cys (DHHC)-12 serves to tether APP in the Golgi and suppresses the generation of APP-containing vesicles, which in turn suppresses the trafficking of APP-containing vesicles into the late secretary pathway. This attenuated generation and transport of APP-containing vesicles down-regulated APP metabolism, including Aβ generation. In addition to this overall suppression of APP trafficking and metabolism by AID/DHHC-12, the mutant AID/DHHC-12 protein, of which palmitoyltransferase activity was impaired, facilitated α-cleavage of APP through the activation of a disintegrin and metalloproteinase 17 (ADAM17), a major α-secretase. Therefore, AID/DHHC-12 regulates APP trafficking and metabolism in multiple ways. Dysregulation of the generation and/or transport of APP-containing vesicles and the α-secretase by AID/DHHC-12 malfunction in neurons may be involved in the early pathogenesis of AD.

Materials and methods

Antibodies

The commercially available antibodies used in this study were purchased as follows: the mouse monoclonal anti-alpha tubulin (Invitrogen, Carlsbad, CA, USA), anti-a N-DYKDDDDK-C protein (FLAG) (M2; Sigma, St Louis, MO, USA), anti-green fluorescence protein (GFP) (1E4; Medical & Biological Laboratories, Nagoya, Japan), anti-APP (22C11; Chemicon, Temecula, CA, USA/Millipore Corporation, Bedford, MA, USA), and anti-sAPPα (2B3; Immuno-Biological Laboratories, Takasaki, Japan) antibodies; rabbit polyclonal anti-RFP (Medical & Biological Laboratories, Nagoya, Japan), anti-APP C-terminal APP/C (A8717; Sigma), and anti-sAPPβ (Immuno-Biological Laboratories) antibodies; and goat polyclonal anti-rabbit and anti-mouse immunoglobulin antibodies conjugated to horseradish peroxidase (GE Healthcare, Little Chalford, UK). A rabbit polyclonal anti-AID/DHHC-12 (UT141) antibody was raised against the glutatione-S-transferase (GST)-fusion of the complete human AID/DHHC-12 sequence and affinity purified with antigen-coupled resin before use; the specificity was examined by immunoblotting (Supplementary Figure S1). Anti-alcadeinα (Alcα) UT131 antibody is equivalent to UT83 for specificity (Araki *et al.* 2003) and the characterization of anti-APP G369 antibody has been described (Oishi *et al.* 1997).

Plasmid construction

A cDNA encoding the entire human AID open reading frame was isolated in a yeast two-hybrid screen from a human brain MATCHMAKER cDNA library (Clontech, Mountain View, CA, USA) using a bait composed of a cDNA encoding the cytoplasmic region of Alcα (amino acids 893–971 of human Alcα1; Araki *et al.* 2003). The cDNA sequence was amplified from cDNA of HEK293 cells with primers (forward: 5′-TACATAGCTAGCATGGCGCCCTGGGCGCTC-3′; reverse: 5′-TACATACTCGAGCTAAACAGCTGGGCTGCT-3′), digested, and cloned into the *Nhe*I/*Xho*I sites in pcDNA3.1 or pcDNA3.1 tagged with FLAG at the amino termini to generate pcDNA3.1-AID and pcDNA3.1-N-FLAG-AID, respectively. The cDNA encoding a mutant AID_{AAHS} was generated by replacing the amino acid sequence 124-DHHC-127 with 124-AAHS-127 using site-directed mutagenesis. The cDNAs encoding AID^{1-177}, AID^{1-163}, AID^{1-141}, AID^{1-97}, AID^{98-267} and $AID_{\Delta DHHC}$ (lacking amino acids AID^{98-141}) were generated by PCR and inserted into the pcDNA3.1 vector to construct pcDNA3.1-C-FLAG-AID^{1-177}, pcDNA3.1-C-FLAG-AID^{1-163}, pcDNA3.1-C-FLAG-AID^{1-141}, pcDNA3.1-C-FLAG-AID^{1-97}, pcDNA3.1-N-FLAG-AID^{98-267}, and pcDNA3.1-N-FLAG-$AID_{\Delta DHHC}$, respectively. The pcDNA3-FLAGAPP695 (Ando *et al.* 1999) and pcDNA3-ADAM17-HA (Endes *et al.* 2005) plasmids have already been described. The pcDNA3.1-APP695Δcyt and pcDNA3.1-$APP695_{N680}$ plasmids encode amino acids 1–651 and 1–680, respectively, of human APP 695.

To facilitate microscopic observation of expressed proteins in living cells, plasmids were prepared to generate proteins of interest fused with a fluorescent protein. The cDNAs encoding AID and AID_{AAHS} were recloned into the *Nhe*I/*Xho*I sites of pcDNA3.1-C-enhanced cyan fluorescent protein (EGFP) and pcDNA3.1-C-monomeric red fluorescent protein (mRFP) or pcDNA3.1-N-EGFP and pcDNA3.1-N-mRFP to generate pcDNA3.1-C-EGFP-AID and pcDNA3.1-C-mRFP-AID or pcDNA3.1-N-EGFP-AID_{AAHS} and pcDNA3.1-N-mRFP-AID_{AAHS}, respectively. The human APP695 cDNA was recloned into the *Eco*RV/*Bam*HI sites of pcDNA3.1-C-mRFP to generate pcDNA3.1-mRFP-APP and into the *Eco*RV/*Bam*HI sites of pcDNA3.1-C-EGFP to generate pcDNA3.1-C-EGFP-APP. The protein product of the pECFP (enhanced cyan fluorescent protein)-Golgi plasmid (BD Biosciences, San Jose, CA, USA) was used as a marker for the trans-medial region of the Golgi.

Immunoblotting and co-immunoprecipitation analysis

Neuro2a (N2a) cells ($\sim 1 \times 10^6$) were transiently transfected with the indicated amount of plasmid using Lipofectamine 2000 (Invitrogen) and cultured for 24 h in medium containing 10% (v/v) fetal bovine serum. Cells were harvested and lysed in a lysis buffer [phosphate-buffered saline (PBS) containing 1% (w/v) sodium dodecyl sulfate (SDS) and 4 M urea] and sonicated. The proteins were separated with 6% (w/v) polyacrylamide gel SDS electrophoresis for APP and secreted large amino-terminal fragments of APP (sAPP), or 15% (w/v) polyacrylamide gel SDS electrophoresis for the carboxyl-terminal fragment of APP cleaved at α- or β- site (APP-CTF) and AID. The proteins within

gels were transferred onto respective membranes and analyzed by immunoblotting with indicated antibodies.

For co-immunoprecipitation analyses, cells were harvested and lysed in HBS-T lysis buffer [10 mM HEPES (pH 7.6) containing 150 mM NaCl, 5 mM EDTA, 0.5% (v/v) Triton X-100, 5 μg/mL chymostatin, 5 μg/mL leupeptin, and 5 μg/mL pepstatin A] and centrifuged for 5 min at 4°C. The resulting supernatants were incubated with the indicated antibodies at 4°C for 2 h. The immunocomplex was recovered with protein G-Sepharose beads (GE Healthcare). In a separate study, the cultured medium of cells was collected and subjected to pre-clearing with protein G-Sepharose beads. The medium was then incubated with an anti-FLAG M2 antibody at 4°C for 2 h. The immunocomplex was recovered with protein G-Sepharose beads.

Cell surface proteins were biotinylated with EZ-Link Sulfo-NHS-LC-Biotin (Thermo Scientific, Walthan, MA, USA) for 30 min on ice, and the reaction was stopped by washing cells with 50 mM Tris–-HCl buffer (pH 7.5). The cells were lysed in a HBS-T and biotinylated proteins were recovered with Immobilized NeutrAvidin Gel (Thermo Scientific, Walthan, MA, USA), and analyzed by immunoblotting. Tubulin was used as a control showing that intracellular protein was not biotinylated.

Microscopic observation of protein localization

Cells cultured on an eight-well or two-well chamber slide glass (Nalge Nunc International, Rochester, NY, USA) were transfected with the indicated plasmids using Lipofectamine 2000 for 24 h, and the intracellular localization of the fluorescent fusion proteins was observed under a confocal laser scanning microscope LSM510 (Carl Zeiss, Oberkochen, Germany) or a fluorescence microscope BZ-9000 (KEYENCE, Osaka, Japan).

Quantitative Analysis of Aβ

Neuro 2a cells ($\sim 1 \times 10^6$) were transiently transfected with pcDNA3-APP695 (0.4 μg) and the indicated plasmid (0.4 μg) and then cultured in Dulbecco's modified Eagle's medium containing 10% (v/v) fetal bovine serum for 32–48 h. Aβ40 and Aβ42 secreted into the medium were quantified by sandwich ELISA as described previously except that 82E1 (Immuno-Biological Laboratories) was used instead of the 2D1 antibody (Tomita *et al.* 1998). Briefly, wells of a 96-well plate were coated with Aβ40 (4D1) or Aβ42 (4D8) end-specific monoclonal antibodies (0.3 μg of IgG in PBS), washed with PBS containing 0.05% (v/v) Tween 20 (PBST), blocked with bovine serum albumin [3% (w/v) in PBS], and washed with PBST. Then a sample (100 μL) diluted suitably with PBST containing 1% (w/v) bovine serum albumin (dilution buffer) was incubated together with a standard amount of synthetic Aβ (1–40) or Aβ (1–42) peptides. After washes, the wells were treated with biotinylated 82E1 (Immuno-Biological Laboratories), washed, and incubated with 100 μL of a streptavidin–horseradish peroxidase complex (1 : 2000 dilution, RPN1051; Amersham Pharmacia Biotech, Piscataway, NJ, USA). The plates were further washed, and 100 μL of 2,2′-azino-bis(3-ethylbenzothiazoline-6-sulfonia acid) or ABTS solution (KPL 5062-01; Kirkegaard & Perry Laboratories Inc., Gaithersburg, MD, USA) was added to the wells. The plates were incubated at 15–25°C and the absorbance at 415 nm was measured.

Results

Interaction of AID/DHHC-12 with Alcadeinα and APP

In a comprehensive yeast two-hybrid screen using the cytoplasmic region of Alcα as a bait, we picked up 500 clones from 9.8×10^6 clones on selective medium lacking tryptophan, leucine, and histidine to assay for the activation of *HIS3* reporter gene. These positive clones were further assayed for the activation of the *lacZ* reporter gene and we picked up 78 clones and determined their nucleotide sequences. Five of 78 clones encoded a novel *tetra*-transmembrane protein containing a DHHC domain. This protein was later identified as DHHC-12, a member of the protein palmitoyltransferase family (reviewed in Mitchell *et al.* 2006), which possesses four transmembrane domains as shown schematically in Fig. 1. The positive interaction between DHHC-12 and the cytoplasmic region of Alcα was confirmed by the activation of *lacZ* reporter gene (Supplementary Figure S2). The protein interaction was confirmed in mammalian cells (Fig. 2). N2a cells were expressed transiently with FLAG-AID and Alcα, and co-immunoprecipitation assay with anti-Alcα antibody recovered FLAG-AID along with Alcα (Fig. 2a), indicating that AID associated with Alcα in mammalian cells.

We further analyzed which region of AID binds to Alcα by performing co-immunoprecipitation assays with cells expressing FLAG-AID proteins and Alcα, and by performing *in vitro* pull-down assays with GST-AID fusion proteins with Alcα. The preliminary results of these assays suggested that the second loop, including the DHHC domain, contains a binding region for the cytoplasmic domain of Alcα, and that the C-terminal region contributed partly to

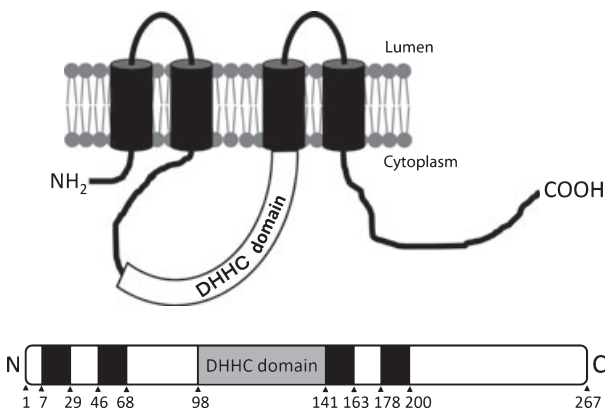

Fig. 1 Schematic structure of AID/DHHC-12. Black cylinders represent the deduced transmembrane domains (amino acid positions; 7–29, 46–68, 141–163, and 178–200). DHHC (amino acid positions 98–140) indicates a domain including a conserved 124-Asp–His–His–Cys-127 motif, which is the palmitoyltransferase catalytic center. Numbers indicate amino acid positions.

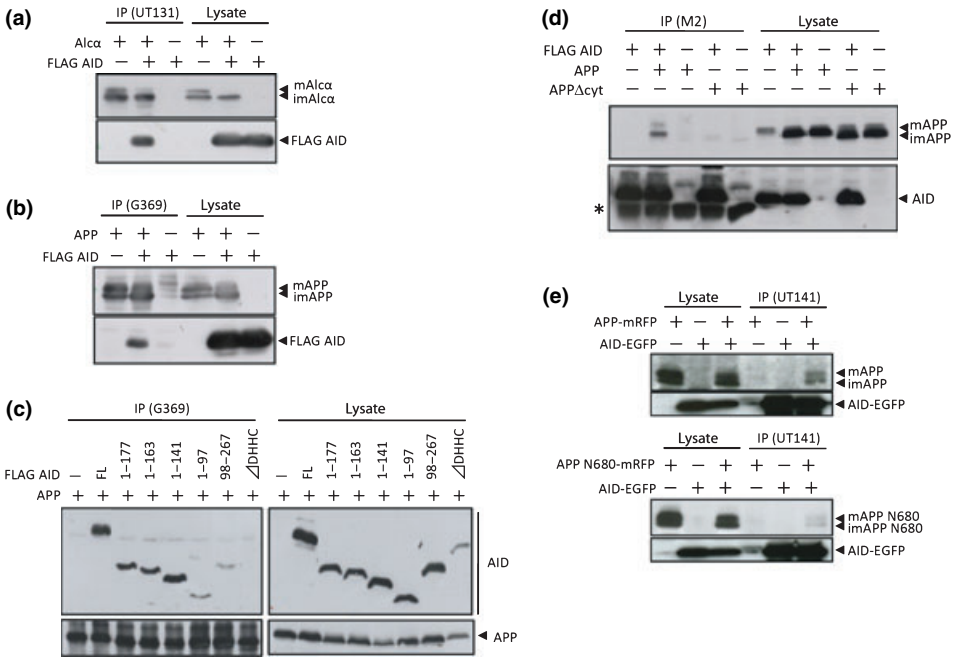

Fig. 2 Interaction of Alcadeinα (Alcα)and APP with AID/DHHC-12. (a, b) Co-immunoprecipitation of Alcα (a) and APP (b) with AID. N2a cells ($\sim 1 \times 10^6$) were transiently transfected with 0.75 μg of pcDNA3.1-hAlcα1 (a) or pcDNA3-APP695 (b) in the presence (+) or absence (−) of pcDNA3.1-N-FLAG-AID (0.75 μg). To standardize the plasmid amount, empty vector (−) was added to yield 1.5 μg of plasmid in total. The cell lysates were subjected to immunoprecipitation with anti-Alcα UT131 (a, upper) and anti-APP G369 (b, upper) antibodies. The immunocomplex was detected by immunoblotting with anti-Alcα UT131 (a, upper) and anti-APP/C (b, upper) antibodies, or anti-FLAG M2 antibody (lower in a and b). The mature Alcadeinα (mAlcα) indicates a slower-migrating form with complex *N*-glycans, and the immature Alcadeinα (imAlcα) indicates a faster-migrating form with high-mannose *N*-glycans (Araki *et al.* 2007). The mature APP (mAPP) indicates a slower-migrating form with *N*- and *O*-glycans, and the immature APP (imAPP) indicates a faster-migrating form with *N*-glycan (reviewed in Suzuki and Nakaya 2008). (c) Co-immunoprecipitation of AID mutant proteins with APP. N2a cells ($\sim 1 \times 10^6$) were transiently transfected with 0.75 μg of pcDNA3.1-C-FLAG-AID (FL), pcDNA3.1-C-FLAG-AID$^{1-177}$ (1–177), pcDNA3.1-C-FLAG-AID$^{1-163}$ (1–163), pcDNA3.1-C-FLAG-AID$^{1-141}$ (1–141), pcDNA3.1-C-FLAG-AID$^{1-97}$ (1–97), pcDNA3.1-N-FLAG-AID$^{98-267}$ (98–267) and pcDNA3.1-N-FLAG-AID$_{\Delta DHHC}$ (ΔDHHC) or pcDNA3.1 vector alone (−) in the presence of 0.75 μg of pcDNA3-APP695 (APP). The cell lysates were subjected to immunoprecipitation with anti-APP G369 antibody. The immunoprecipitate (IP) and cell lysate (lysate) were analyzed by immunoblot analysis with anti-FLAG M2 or anti-APP/C antibodies. (d) Failure of APPΔcyt to associate with AID/DHHC-12. N2a cells ($\sim 1 \times 10^6$) were transiently transfected with 0.75 μg of pcDNA3.1-N-FLAG-AID along with 0.75 μg of pcDNA3-APP695 (APP) or pcDNA3.1-APP695Δcyt (APPΔcyt). To standardize the plasmid amount, empty vector was added to yield 1.5 μg of plasmid in total. A cell lysate was immunoprecipitated with anti-FLAG antibody M2. The immunoprecipitates (IP) and lysate were analyzed by immunoblotting with anti-APP 22C11 (upper) and anti-FLAG M2 (lower) antibodies. mAPP, mature APP; imAPP, immature APP. Asterisk (*) indicates an IgG light chain in an immunocomplex. (e) Ineffective binding of APP$_{N680}$ to AID/DHHC-12. N2a cells ($\sim 1 \times 10^6$) were transiently transfected with 0.75 μg of pcDNA3.1-AID-EGFP along with 0.75 μg of pcDNA3.1-APP695-mRFP (APP-mRFP) or pcDNA3.1-APP695$_{N680}$-mRFP (APP$_{N680}$-mRFP). To standardize the amount of plasmid used, the empty vector was added to yield a final amount of 1.5 μg of plasmid in all assays. A cell lysate was immunoprecipitated with anti-AID UT141 antibody. The immunoprecipitates (IP) and lysate were analyzed by immunoblotting with anti-EGFP and anti-mRFP antibodies.

the interaction (data not shown). We found that Alcα metabolism was stabilized in cells expressing AID, resulting in an increase in immature Alcα (imAlcα, high manose form) and a decrease in mature Alcα (mAlcα, complexed *N*-glycan form) (Fig. 2a), along with decreases in intracellular AlcαCTF and the amount of sAlcα secreted into the medium (Supplementary Figure S3). Because the physiological function and relevance of Alcα metabolites to AD pathobiology has not been well characterized, we asked whether AID could bind to APP and regulate APP metabolism, which is considered to be an important aspect of the pathogenesis of AD.

Amyloid β-protein precursor and Alc sometimes interact with similar proteins; X11 family proteins associate with both APP and Alc, while JNK-interacting protein 1 binds to APP alone and kinesin light chain (KLC) binds to Alc alone (reviewed in Suzuki and Nakaya 2008; Taru *et al.* 2002; Araki *et al.* 2007), we next examined whether AID associates with APP. N2a cells were expressed transiently with FLAG-AID and APP, and interestingly the co-immunopre-

cipitation assay with anti-APP antibody recovered FLAG-AID along with APP (Fig. 2b), indicating that AID also associated with APP in cells, as did Alcα. The interaction of endogenous APP with AID that expressed at lower levels was confirmed (Supplementary Figure S4a). To detect endogenous APP under the lower level of AID expression, three-times numbers of N2a cells were transfected with a smaller amount of pcDNA3-AID (0.1–1.0 μg) when compared with Fig. 2b, and co-immunoprecipitation study was performed with anti-AID UT141 antibody. The immunoprecipitates were analyzed by immunoblotting with anti-APP/C and UT141 antibodies. Endogenous APP was also recovered with AID expressed at lower level, suggesting that the interaction between APP and AID is a physiologically convincing event but not an artifact by excess expression of proteins. Therefore, we concentrated our analysis of AID on its effect on APP metabolism.

Both the amino- and carboxy-terminal regions of AID/DHHC-12 are located in the cytoplasm, as is second loop containing the DHHC domain. The first and the third loops are located in the lumen (Fig. 1). Therefore, the regions of AID/DHHC-12 that interact with the cytoplasmic region of APP are probably located in its N- and C-terminal regions and/or its second loop, and preliminary studies of Alcα binding to AID have suggested that the most likely regions of interaction are located in the second loop and C-terminal region. We expressed several AID proteins carrying various deletions in N2a cells and performed co-immunoprecipitation assays with anti-APP antibody, although we could not exclude the possibility that domain-deletions in the membrane spanning protein would disturb the overall conformation of AID and make the results difficult to interpret. FLAG-AID$^{1-177}$, FLAG-AID$^{1-163}$, and FLAG-AID$^{1-141}$ associated with APP equally well as did full-length FLAG-AID, while FLAG-AID$^{1-97}$ and FLAG-AID$^{98-267}$ associated weakly with APP. Although the expression of FLAG-AID$_{\Delta DHHC}$ was weak because this mutant may be susceptible to proteolysis, APP seemed not to bind to FLAG-AID$_{\Delta DHHC}$ (Fig. 2c). These data suggest that the DHHC domain may be a major region for APP-binding. However, the AID construct lacking the DHHC domain, FLAG-AID$^{1-97}$, bound to APP as well as the AID construct containing the DHHC domain, FLAG-AID$^{98-267}$, indicating that the binding site in this region may not be contiguous or that the deletion constructs lacked the correct conformation for the interaction with APP.

Thus, we tried to confirm whether the cytoplasmic region of APP is involved in its association with AID/DHHC-12. FLAG-tagged AID was co-expressed with APP lacking its cytoplasmic region (APPΔcyt) in N2a cells, and co-immunoprecipitation assay with anti-FLAG antibody was performed. The anti-FLAG antibody failed to recover APPΔcyt together with FLAG-AID, although it recovered APP (Fig. 2d), indicating that the APP cytoplasmic region is indispensable for the association with AID. Because a recent report revealed that the cytoplasmic tail of APP associates with the membrane (Beel *et al.* 2008), we decided to test if APP interacts with a sequence adjacent to the transmembrane regions of AID. We examined the interaction of AID with APP$_{N680,}$ which lacks the C-terminal 15 amino acids, including the protein interaction motif 681-GYENPTY-687 and the cytoplasmic tail. Cells expressing AID-EGFP with APP-mRFP or APP$_{N680}$-mRFP were lyzed and subjected to the co-immunoprecipitation assay with anti-EGFP antibody. The antibody recovered APP-mRFP with AID-EGFP, but the recovery of APP$_{N680}$-mRFP was very low or null (Fig. 2e). This result suggests that the C-terminal 15 amino acids of APP are important for binding to AID.

To examine the specificity of APP-binding by AID/DHHC-12, we prepared other DHHC proteins and performed co-immunoprecipitation assay with APP. Some of DHHC proteins associated with APP and the remaining members did not bind to APP (unpublished observation, and examples are shown in Supplementary Figure S5, in which DHHC-17 associated with APP as did AID/DHHC-12 while DHHC-20 did not associate with APP), suggesting that some, but not all, of DHHC family proteins, such as AID/DHHC-12 and DHHC-17 bind to APP.

Suppression of APP metabolism by AID/DHHC-12

We next tested whether AID/DHHC-12 regulates APP metabolism. We expressed N-FLAG-APP in N2a cells with or without AID/DHHC-12 and analyzed the intracellular levels of APP and APP-CTF (CTFα and CTFβ, the CFT of APP cleaved at the α- or β-site) and the secretion of sAPP (sAPPα and sAPPβ, sAPP cleaved at the α- or β-site). The expression of APP695 wild-type was used to quantify secreted Aβ40 and Aβ42. In the presence of AID/DHHC-12, mature APP (mAPP, *N*- and *O*-glycosylated APP located in the *trans*-Golgi and late secretary pathway) decreased; in contrast, immature APP (imAPP, *N*-glycosylated APP located in the endoplasmic reticulum and *cis*-/*medial*-Golgi) accumulated in cells, and secretion of sAPPα and sAPPβ decreased (Fig. 3). Given that primary cleavage of mAPP at the α- and β-sites is thought to occur in the secretary pathway after the *trans*-Golgi network (TGN) (reviewed by Small and Gandy 2006; Thinakaran and Koo 2008), the results suggest that over-expression of AID/DHHC-12 retained APP in the early Golgi and suppressed transport of APP into the late secretary pathway. This result was confirmed for endogenous APP. Endogenous mAPP decreased and imAPP accumulated in dose dependent-expression manner of AID. Maturation of endogenous Alcα was also suppressed in cells expressed AID (Supplementary Figure S4b and c). These observations support the idea that AID/DHHC-12 retained APP and Alc in the early Golgi, and suggest that the suppressed maturation of APP, which indicates a suppressed transport of APP into the late

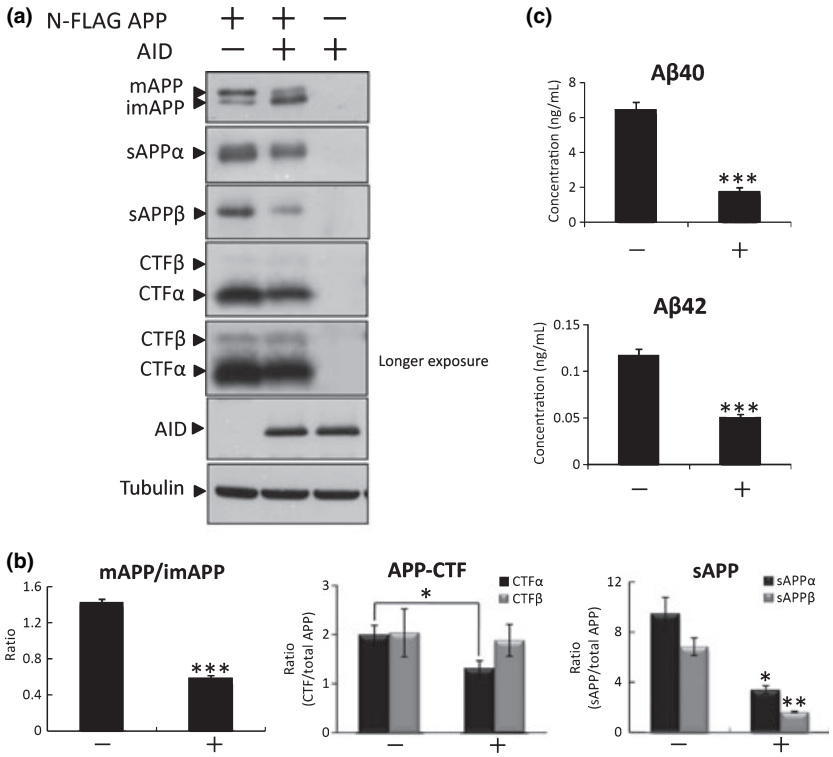

Fig. 3 Suppression of APP metabolism in cells expressing AID/DHHC-12. (a) Changes of APP metabolism by AID expression. N2a cells ($\sim 1 \times 10^6$) were transiently transfected with (+) or without (−) pcDNA3-FLAG-APP695 (0.4 μg) in the presence (+) or absence (−) of pcDNA3.1-AID (0.4 μg). To standardize the plasmid amount, empty vector was added (−) to yield 0.8 μg of plasmid in total. A cell lysate (100 μg protein) was analyzed by immunoblotting with anti-APP cytoplasmic region (APP/C) to detect APP and CTFs, anti-AID (UT141), and anti-tubulin antibodies. Cultured medium (400 μL) was immunoprecipitated with an anti-FLAG (M2) antibody, and the precipitates were analyzed by immunoblotting with anti-sAPPα and anti-sAPPβ antibodies to measure secreted APP (sAPP). (b) Quantification of APP and its metabolites. Proteins detected with ECL were quantified with the VersaDoc imaging analyzer and standardized by the amount of tubulin. Ratios of mAPP/imAPP, APP-CTFα/total APP, APP-CTFβ/total APP, sAPPα/total APP, and sAPPβ/total APP are indicated. APP and sAPP were analyzed with 6% polyacrylamide gel while CTFs are analyzed with 15% polyacrylamide gel, and the proteins separated on both gels are transferred onto the respective nitrocellulose membranes and analyzed by immunoblotting. Therefore, the ratio of APP-CTF/total APP is an arbitrary. +, AID; −, empty vector. Results are shown as mean ± SE ($n = 4$). Data were analyzed by Student's *t*-test (*$p < 0.05$; **$p < 0.005$; ***$p < 0.0005$). Quantitative accuracy of the amount of APP-CTFs detected by immunoblot analysis is shown in Supplementary Figure S6. (c) Suppression of Aβ generation by AID expression. Aβ40 and Aβ42 secreted into the medium of N2a cells ($\sim 1 \times 10^6$) transiently transfected with pcDNA3-APP695 (0.4 μg) in the presence (+) or absence (−) of pcDNA3.1-AID were quantified with sandwich ELISA. Concentrations of Aβ40 and Aβ42 are shown as means ± SE ($n = 3$). Data were analyzed by Student's *t*-test (***$p < 0.0005$).

secretary pathway, in the presence of AID is not an artifact by excess expression of proteins.

Both sAPPα and sAPPβ levels decreased when AID/DHHC-12 was over-expressed. However, only intracellular level of CTFα decreased slightly and the CTFβ level did not decrease when AID/DHHC-12 was over-expressed. The quantification of CTFα and CTFβ was performed within linear range with 100 μg protein of cell lysate (Supplementary Figure S6). This contradiction observed in sAPPβ and CTFβ levels may be interpreted by the further suppression of intracellular secondary γ-site cleavage of CTFβ by the over-expression of AID/DHHC-12. Suppression of the secondary γ-cleavage of APP-CTFβ was examined by measuring the secretion of Aβ from cells over-expressing AID/DHHC-12. Levels of both Aβ40 and Aβ42 were suppressed in cells expressing AID/DHHC-12 (Fig. 3c), suggesting that overall APP metabolism including γ-cleavage is likely to be suppressed by AID/DHHC-12. The results suggest that production of CTFβ decreased but cleavage of CTFβ by γ-secretase is also decreased in cells over-expressing AID/DHHC-12. Therefore, intracellular levels of APP CTFβ in the cells over-expressing AID/DHHC-12 were seemed to be equivalent to those in the cells without expression of AID/DHHC-12. Because α-secretase activity is selectively suppressed by AID/DHHC-12 rather than β-secretase (see Fig. 5 and discussed later), a further decrease of CTFα might be

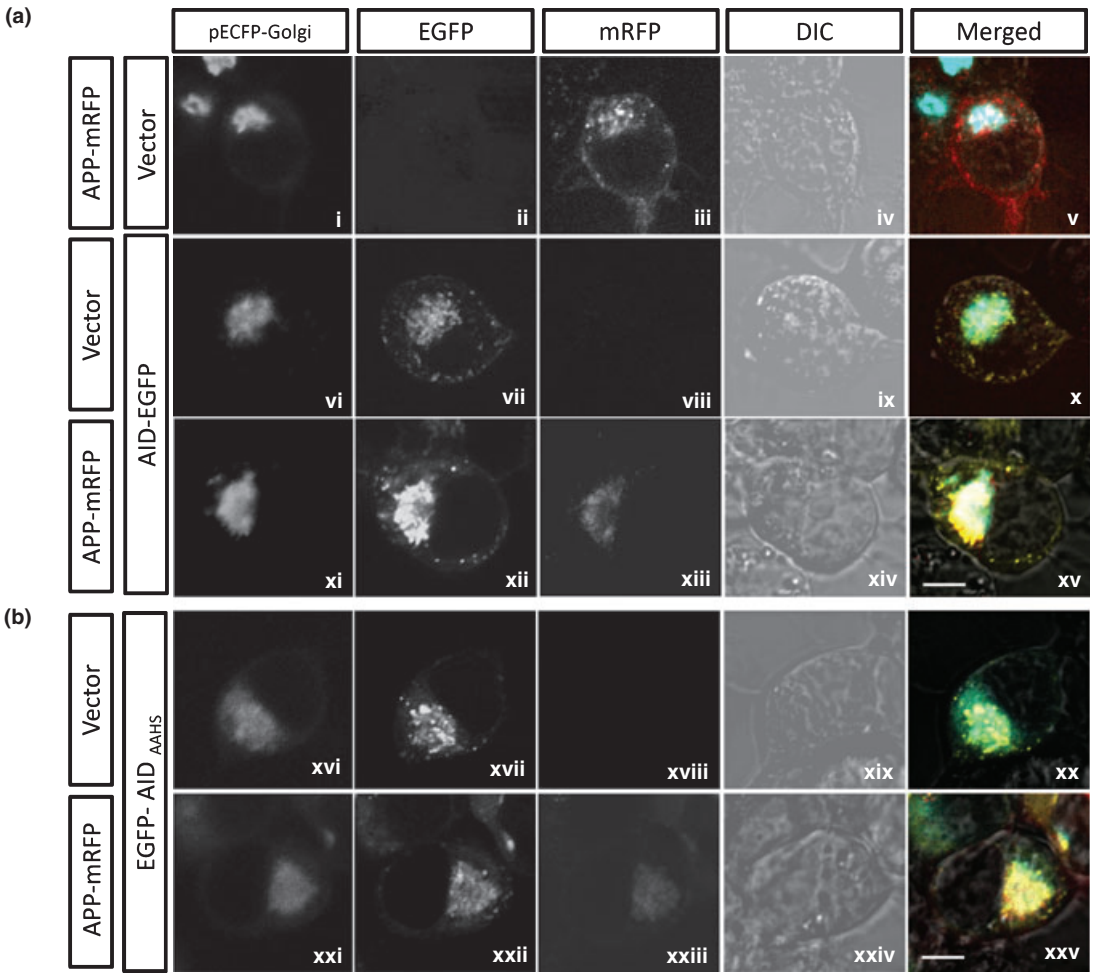

Fig. 4 Intracellular localization of APP and AID/DHHC-12. (a) Localization of APP and AID. N2a cells ($\sim 1 \times 10^5$) were transiently transfected with pcDNA3.1-C-mRFP-APP (0.1 μg, i–v), pcDNA3.1-C-EGFP-AID (0.1 μg, vi–x), or a combination of pcDNA3.1-C-mRFP-APP (0.1 μg) and pcDNA3.1-C-EGFP-AID (0.1 μg) (xi–xv), in the presence of pECFP-Golgi (0.1 μg). DIC indicates Differential Interference Contrast microscopy (iv, ix, xiv) and the signals are merged in the rightmost rows (v, x, xv). Scale bar, 5 μm. (b) Localization of APP and AID_{AAHS}. N2a cells ($\sim 1 \times 10^5$) were transiently transfected with pcDNA3.1-N-EGFP-AID_{AAHS} (0.1 μg) in the presence (xxi–xxv) or absence (xvi–xx) of pcDNA3.1-C-mRFP-APP (0.1 μg) together with pECFP-Golgi (0.1 μg). DIC (xix, xxiv) and the merged images (xx, xxv) are indicated. Scale bar, 5 μm.

observed when compared with the level of CTFβ. Although we cannot exclude other possibilities, one of significant functions of AID/DHHC-12 is thought to be an overall decrease of APP metabolism by suppression of APP trafficking.

To examine whether AID/DHHC-12 tethers APP in the Golgi, thereby suppressing the generation of APP-containing vesicles and preventing them from being sent to the late secretary pathway, we co-expressed APP-mRFP and AID-EGFP in N2a cells and examined their localization with confocal microscopy (Fig. 4a). The Golgi was visualized by co-transfection of pECFP-Golgi, whose encoded protein localizes in the *medial-/trans*-Golgi (panels i, vi, xi). APP and AID largely localized in the Golgi and in small cytoplasmic vesicles together with plasma membrane (APP, panels i–v; AID, panels vi–x), in agreement with a report showing that DHHC-12 is largely located in Golgi (Ohno *et al.* 2006). APP is also to reside largely in Golgi; however, APP in cells co-expressed with AID is further concentrated in the Golgi, and the cytoplasmic small vesicles containing APP almost disappeared (panels xi–xv). The Golgi localization of APP and AID was further confirmed by immunostaining of endogenous GM130, a *cis*-Golgi matrix protein, in cells expressing APP-mRFP and AID-EGFP (Supplementary Figure S7). These observations suggest that AID/DHHC-12 suppresses the generation and/or trafficking of APP-containing vesicles that would normally enter into the late secretary pathway.

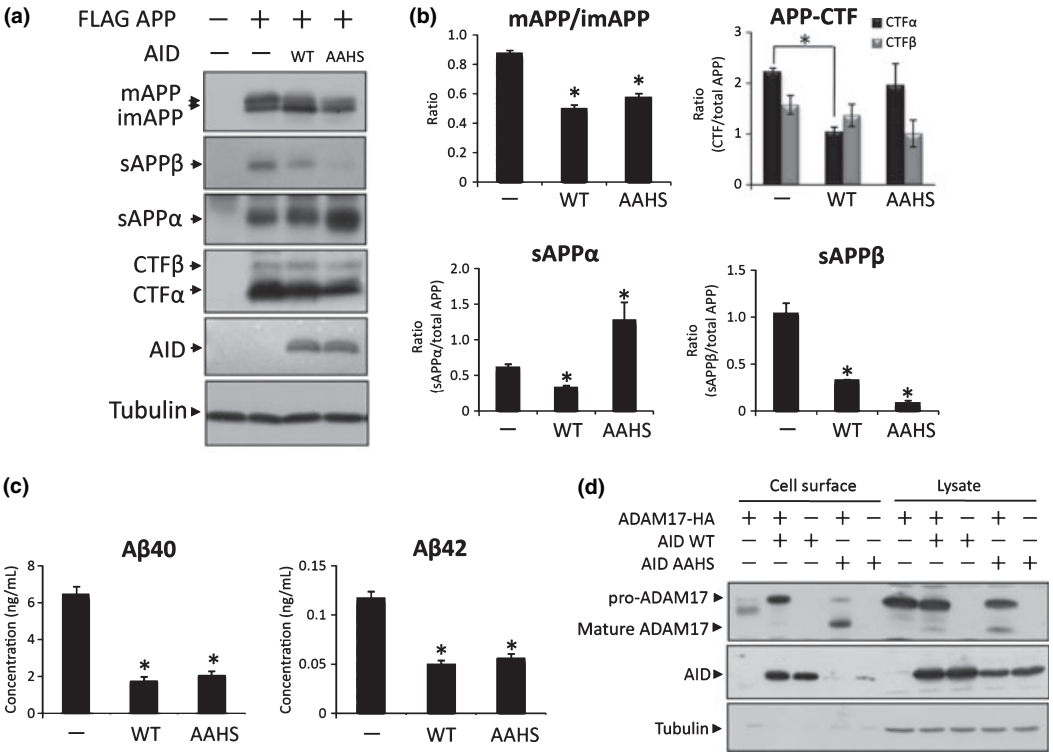

Fig. 5 AID DHHC motif–independent suppression of APP metabolism and -dependent facilitation of APP α-cleavage. (a) Effect of AID and AID_{AAHS} in APP metabolism. N2a cells (~1×10^6) were transiently transfected with pcDNA3-FLAG-APP695 (0.4 μg) in the presence (+) of 0.4 μg of pcDNA3.1-N-FLAG-AID (WT) or pcDNA3.1-N-FLAG-AID_{AAHS} (AAHS). To standardize the plasmid amount, empty vector was added (–) to yield 0.8 μg of plasmid in total. A cell lysate (100 μg protein) was analyzed by immunoblotting with an anti-FLAG M2 antibody to detect APP and AID, or an anti-APP/C antibody to detect APP-CTF. Cultured medium (400 μL) was immunoprecipitated with M2 and the precipitates were analyzed for secreted APP (sAPP) by immunoblotting with anti-sAPPα and anti-sAPPβ antibodies. (b) Quantification of APP metabolites. Proteins detected with ECL were quantified with a VersaDoc imaging analyzer and standardized by the amount of tubulin. Ratios of mAPP/imAPP, APPCTFα/total APP, APPCTFβ/total APP, sAPPα/total APP, and sAPPβ/total APP are indicated as described in the legend of Fig. 3b. Results are shown as mean ± SE ($n = 3$). Data were analyzed by one-way analysis of variance followed by Tukey's test (*$p < 0.05$). (c) Effect of AID and AID_{AAHS} on Aβ generation. N2a cells (~1×10^6) were transiently transfected with pcDNA3-APP695 (0.4 μg) in the presence or absence (–, empty vector alone) of 0.4 μg of pcDNA3.1-N-FLAG-AID (WT) or pcDNA3.1-N-FLAG-AID_{AAHS} (AAHS). The concentrations of Aβ40 and Aβ42 are shown as means ± SE ($n = 3$). The data were analyzed by one-way analysis of variance followed by Tukey's test (*$p < 0.05$). (d) Increased cleavage of pro-ADAM17 in cells expressing AID_{AAHS} but not AID_{WT}. N2a cells (~1×10^6) were transiently transfected with pcDNA3-ADAM17-HA (0.75 μg) in the presence or absence (–, empty vector alone) of 0.75 μg of pcDNA3.1-N-FLAG-AID (WT) or pcDNA3.1-N-FLAG-AID_{AAHS} (AAHS). To standardize the plasmid amount, empty vector was added to yield 1.5 μg of plasmid in total. Cell surface biotinylated proteins (Cell surface) and crude lysates (lysate, 100 μg protein) were analyzed by immunoblotting with anti-HA (upper), anti-FLAG (middle) and anti-tubulin (lower) antibodies. Arrowheads indicate pro-ADAM17-HA (134 kDa) and mature ADAM17-HA (98 kDa) in upper row.

AID DHHC motif–independent suppression of metabolism, trafficking of APP and AID DHHC-dependent facilitation of α-cleavage of APP

DHHC proteins are palmitoyltransferases, and the DHHC motif is essential for the enzymatic activity (reviewed in Mitchell *et al.* 2006). We examined whether AID/DHHC-12 needs its enzymatic activity to suppress APP metabolism by replacing the amino acid sequence of DHHC with AAHS. We co-expressed N-FLAG-APP with the mutant AID (AID_{AAHS}) or wild-type AID (AID_{WT}) in N2a cells, and compared APP metabolism, including Aβ secretion. Except for sAPPα generation, AID_{AAHS} produced effects identical to those of AID_{WT} in APP metabolism: the accumulation of imAPP, decrease of sAPPβ secretion, and suppression of Aβ secretion (Fig. 5a–c). Interestingly, AID_{AAHS} facilitated non-amyloidogenic α-cleavage and increased sAPPα secretion (Fig. 5a and b). CTFα did not decrease significantly in cells expressing AID_{AAHS} as it did in cells expressing AID_{WT}. The quantification of CTFα and CTFβ was performed within the linear range (Supplementary Figure S6). The α-secretase activity may be suppressed by palmitoylation of the α-secretase itself or of other unidentified molecules involved in the regulation

of α-secretase activity. Because one of major α-secretase is ADAM17 (Buxbaum *et al.* 1998), we asked whether AID_{AAHS} facilitates the activation of ADAM17. N2a cells were expressed with C-terminally hemagultinin (HA)-tagged ADAM17 (ADAM17-HA) in the presence of AID_{WT} or AID_{AAHS} (Fig. 5d). To assess if these proteins are transported to plasma membrane, the cell surface proteins were biotinylated, solubilized, and recovered with NeutrAvidin beads (Pierce, Rockford, IL, USA). The labeled proteins and cell lyates were analyzed by immunoblotting with anti-HA, anti-AID, and anti-tubulin antibodies. Interestingly, cells expressing AID_{AAHS} increased mature ADAM17 (lysate of Fig. 5d), which was generated by a proteolytic removal of N-terminal pro-domain (reviewed by Thomas 2002). This mature ADAM17 was predominantly localized on cell surface in the presence of $AID_{AAHS,}$ while immature pro-ADAM17 was dominant in cells expressing AID_{WT} (cell surface and lysate of Fig. 5d). In the absence of exogenous AID, excess amount of pro-ADAM17 was also reproducibly decreased on cell surface by metabolic degradation along with less mature ADAM17. Very interestingly, AID_{WT} but not AID_{AAHS} was also detected on cell surface. This may indicate that an excess expression of AID_{WT} suppresses the proteolytic cleavage of pro-ADAM17 and enhances its localization on plasma membrane together with AID_{WT}, although ADAM17 does not associate with AID (data not shown) and the detailed mechanism to suppress the ADAM17 activation by AID is a future issue to be revealed. Because maturation/activation of ADAM17 occurs in late secretary pathway (reviewed by Thomas 2002), AID functions to suppress the activation of ADAM and AID_{AAHS} may function as an enzymatic dominant-negative form to endogenous AID molecules. Although further studies will be needed to reveal the role of AID in the regulation of ADAM activation, the present data suggest that AID possesses a function in ADAM regulation independent of the overall suppression of APP trafficking and metabolism.

We also examined the cellular distribution of AID_{AAHS} and APP in N2a cells expressing EGFP-AID_{AAHS} and APP-mRFP (Fig. 4b). The cellular distribution of AID_{AAHS} expressed alone was largely within the Golgi together with the small cytoplasmic vesicles, which were similar to that of AID_{WT} (compare panels xvi–xx in b to vi–x in a of Fig. 4). However, the plasma membrane localization of AID_{AAHS} decreased when compare with AID_{WT} (compare panel vii in a with xvii in b of Fig. 4), which agree with the result that only extremely small amount of AID_{AAHS} can locate on plasma membrane (Fig. 5d). APP was also tethered within the Golgi in the presence of AID_{AAHS}, and APP-containing vesicles disappeared from the cytoplasm as it was with AID_{WT} (compare panels xiii in a and xxiii in b to iii in a of Fig. 4). The intracellular localizations of AID_{WT} and AID_{AAHS} along with APP were also confirmed by immunostaining of GM130 in cells expressing AID_{WT}-EGFP or EGFP-AID_{AAHS} with APP-mRFP (Supplementary Figure S7). The results suggest that the effects of AID in suppressing APP metabolism, and tethering APP within the Golgi are independent of the DHHC domain, which indicate an independent function of palmitoyltransferase activity.

Generation of APP-containing vesicles from Golgi and their movement were confirmed in living cells. The

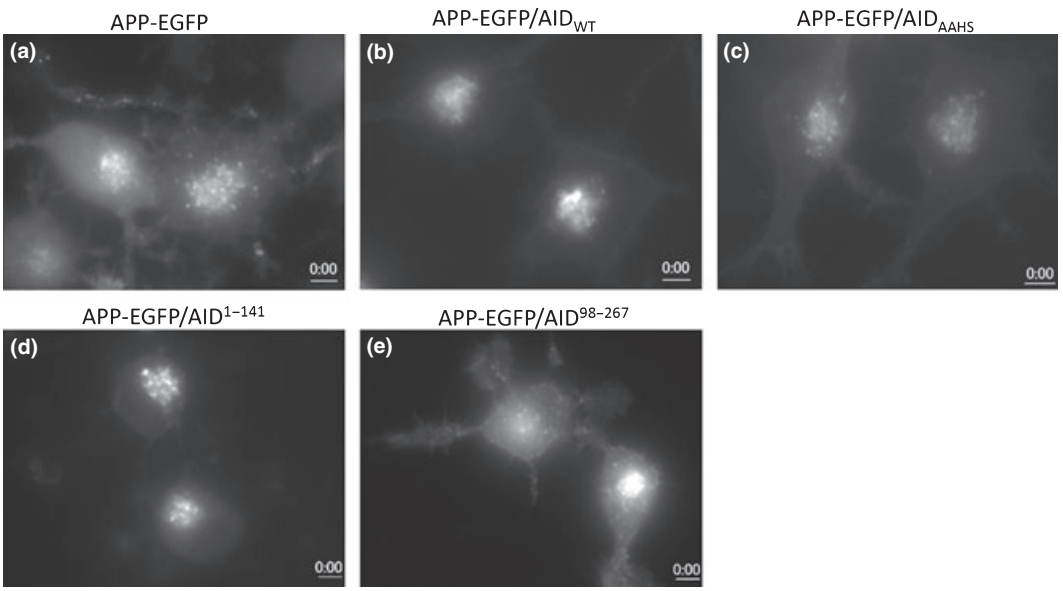

Fig. 6 Generation and movement of APP-containing vesicles in living N2a cells over-expressing AID. N2a cells (~1×10^5) were transiently transfected with 0.15 μg of pcDNA3.1-APP-EGFP and 0.15 μg of pcDNA3.1-AID (b), pcDNA3.1-AID_{AAHS} (c), pcDNA3.1-C-FLAF-AID^{1-141} (d), pcDNA3.1-N-FLAG-AID^{98-267} (e) or vector alone (a). The generation and movement of APP-containing vesicles were observed with fluorescence microscope, BZ-9000 (see Supplementary Movie S1). Scale bar, 5 μm.

movement of APP-containing vesicles in N2a cells expressing APP-EGFP with AID_{WT} or AID_{AAHS} was analyzed (Fig. 6 and supplementary Movie S1). In N2a cells expressing APP-EGFP alone, APP-containing vesicles with a strong fluorescent signal were observed moving away from their site of generation in the Golgi (panel a, see the vesicles located at distal regions of cell body). However, the moving APP-containing vesicles distributed throughout cell remarkably decreased in cells expressing APP-EGFP in the presence of AID_{WT} or AID_{AAHS} (panels b and c, and also compare Movie S1a with Movie S1b and c). APP-EGFP was further analyzed in cells expressing AID^{1-141}, which has normal APP-binding activity, and in cells expressing AID^{98-267}, which has reduced binding activity for APP (see panels d and e, Fig. 2c for binding, and also Movie S1d and e). AID^{1-141} decreased the level of APP-containing vesicles as did AID_{WT}, while AID^{98-267} did not. Taken together, these findings indicate that AID/DHHC-12 is likely to tether APP in the Golgi in an enzyme activity-independent manner that is perhaps dependent on APP-binding. This would inhibit the generation of APP-containing vesicles and suppress the trafficking of these vesicles into the late secretary pathway.

Discussion

Generation of Aβ is a major cause of AD pathogenesis that is closely related to intracellular trafficking of APP (reviewed in Suzuki *et al.* 2006; Small and Gandy 2006; Suzuki and Nakaya 2008). Aβ is generated from mAPP by serial cleavage by β- and γ-secretases in the late secretary pathway, after the Golgi and TGN in which APP maturation is completed (Tomita *et al.* 1998). In fact, BACE, the primary enzyme that cleaves APP to generate Aβ, is active in the late secretory pathway from the TGN and endosomes to the plasma membrane (Small and Gandy 2006; Thinakaran and Koo 2008). Furthermore, disruption of axonal anterograde transport of APP-containing vesicles causes a trafficking backlog and enhances the generation of Aβ in neuronal cells (Stokin *et al.* 2005; Araki *et al.* 2007). Thus, revealing the molecular mechanisms that regulate the generation of APP-containing vesicles at the Golgi and their trafficking into the late secretory pathway will be important for understanding the regulation of Aβ generation in cells.

To confirm the physiological function of endogenous AID/DHHC-12, we tried to establish cell lines in which the expression of endogenous AID/DHHC-12 was knocked down by an small-interference RNA targeting AID. Unfortunately, despite several attempts we failed to establish such cell lines and therefore could not examine the metabolism of APP and the trafficking of APP-containing vesicles in AID-deficient cells. Cells with suppressed AID/DHHC-12 expression may have a defect in the regulation of the protein secretory pathway that renders them unable to grow.

We found that the suppression of APP metabolism, including Aβ generation, by AID/DHHC-12 is a result of attenuated entrance of APP-containing vesicles into the late secretory pathway following the Golgi. Therefore, one of the major functions of AID/DHHC-12 is to retain membrane proteins like APP in the Golgi, and an as-yet-unknown mechanism regulating AID/DHHC-12 may allow the generation and/or release of APP-containing vesicles. We first hypothesized that one likely mechanism of regulation would be DHHC-dependent enzyme activity, because DHHC family proteins are palmitoyltransferases, some of which mediate protein–membrane interactions and the subcellular trafficking of proteins (Fukata *et al.* 2004). The enzyme reaction to transfer the palmitate to the protein is dependent on the DHHC motif (Roth *et al.* 2002). Although the substrates of DHHC-12 remain unclear, APP does not contain the necessary acceptor amino acid, a cysteine residue, in its cytoplasmic region. Moreover, the AID mutant carrying the AAHS sequence instead of DHHC tethered APP at the Golgi just as much as the wild-type AID/DHHC-12. Therefore, we concluded that AID/DHHC-12 functions in the tethering of APP at Golgi regardless of its palmitoyltransferase activity. An alternate explanation may be that the enzyme activity of AID/DHHC-12 is usually masked in the physiological condition when endogenous AID/DHHC-12 becomes enzymatically active in response to some stimulus, more APP may begin to traffic into the late secretary pathway from the Golgi. Verification of such hypothesis on regulatory mechanism of APP trafficking is future issue after identification of target molecule(s) palmitoylated by AID/DHHC-12.

The intracellular level of CTFα decreased slightly when AID/DHHC-12 was over-expressed, whereas the CTFβ level did not change remarkably. APP-CTF is decreased by the suppression of the primary cleavage and is not subjected to further cleavage by the suppression of intramembrane secondary γ-site cleavage by the result of overall suppression of APP trafficking and metabolism, which induces accumulation of CTF in cells expressing AID/DHHC-12. Thus, the total intracellular levels of APP-CTFα and CTFβ seemed to be equivalent in cells over-expressing AID/DHHC-12, regardless of the decreased level of sAPPα and sAPPβ. However, interestingly, α-secretase activity appeared to be suppressed by AID_{WT} and enhanced by AID_{AAHS}. Thus, it is possible to discuss that decrease of CTFα is because of a further suppression of APP α-cleavage in cells over-expressing AID_{WT}. The major α-secretases are ADAM10 and ADAM17 (Buxbaum *et al.* 1998; Lammich *et al.* 1999; Allinson *et al.* 2003), which are type I membrane proteins with cytoplasmic regions containing one cysteine residue. The palmitoylation of ADAM10 and ADAM17 or a regulatory factor of either ADAM10 or ADAM17 may inactivate their maturation process. Indeed, we found that AID_{WT} stabilized pro-ADAM17 while AID_{AAHS} induced the

activation of ADAM17. Although further analysis is needed to reveal the regulatory mechanism of α-secretase activity, including ADAM17, these observations suggest that AID/DHHC-12 plays an important role in the regulation of α-secretase activity, which differs from another activity that AID/DHHC-12 suppresses overall trafficking and metabolism of APP in enzymatic activity-independent manner.

The DHHC protein family is composed of 23 proteins, and at least one-third of them are reported to localize largely in the Golgi (Ohno *et al.* 2006). Another DHHC protein in addition to AID/DHHC-12 has been reported to suppress the trafficking of membrane proteins from the Golgi: Golgi-specific DHHC zinc finger protein (GODZ)/DHHC-3 suppresses the sorting of the glutamate receptor GluRα1 from the Golgi, although the mechanism has not been analyzed in detail (Fang *et al.* 2006). It is therefore possible that different DHHC proteins regulate the generation and trafficking of vesicles containing a variety of membrane proteins from the Golgi. Our finding that AID/DHHC-12 is one of the molecules to regulate APP trafficking from Golgi sheds light on the mechanism of intracellular APP trafficking, and may further the development of drugs to suppress Aβ generation, together with a finding that AID/DHHC-12 regulates non-amyloidogenic α-secretase activity.

Acknowledgments

We thank Drs. A. Miyawaki (RIKEN, BSI, Japan), F. Fahrenholz (Johannes Gutengerg-University, German), S. Gandy (Mount Scinai School of Medicine, USA), and A. Kihara (Hokkaido University) for supplying materials. This work was supported by Grants-in-Aid for Scientific Research 20023001 (TS), 207900018 (TS), and 207900049 (TN) from the Ministry of Education, Science, Culture, Sports, and Technology, Japan. CM and YS are the recipient of research fellowships from the Japan Society for the Promotion of Science for young scientists.

Supporting Information

Additional Supporting Information may be found in the online version of this article:

Figure S1. Specificity of anti-AID/DHHC-12 antibody.

Figure S2. Interaction of AID/DHHC-12 with the cytoplasmic region of Alcα.

Figure S3. Suppression of Alcα metabolism by AID.

Figure S4. Interaction of endogenous APP with AID/DHHC-12 that expressed at lower level, and alterations of endogenous APP and Alcα maturation by expression of AID/DHHC-12.

Figure S5. Interaction of DHHC family proteins with APP.

Figure S6. Quantitative accuracy of the amount of APP-CTFs detected by immunoblot analysis with anti-APP C-terminal antibody.

Figure S7. Intracellular localization of APP and AID/DHHC-12.

Movie S1. Generation and movement of APP-containing vesicles in living N2a cells over-expressing AID or AID mutants.

As a service to our authors and readers, this journal provides supporting information supplied by the authors. Such materials are peer-reviewed and may be re-organized for online delivery, but are not copy-edited or typeset. Technical support issues arising from supporting information (other than missing files) should be addressed to the authors.

References

Allinson T. M. J., Parkin E. T., Turner A. J. and Hooper N. M. (2003) ADAMs family members as amyloid precursor protein α-secretases. *J. Neurosci. Res.* **74**, 342–352.

Anderson O. M., Reiche J., Schmidt V. *et al.* (2005) Neuronal sorting protein-related receptor sorLA/LR11 regulates processing of the amyloid precursor protein. *Proc. Natl Acad. Sci. USA* **102**, 13461–13466.

Ando K., Oishi M., Takeda S., Iijima K., Isohara T., Nairn A. C., Kirino Y., Greengard P. and Suzuki T. (1999) Role of phosphorylation of Alzheimer's amyloid precursor protein during neuronal differentiation. *J. Neurosci.* **19**, 4421–4427.

Araki Y., Tomita S., Yamaguchi H., Miyagi N., Sumioka A., Kirino Y. and Suzuki T. (2003) Novel cadherin-related membrane proteins, Alcadeins, enhance the X11-like protein-mediated stabilization of amyloid β-protein precursor metabolism. *J. Biol. Chem.* **278**, 49448–49458.

Araki Y., Kawano T., Taru H. *et al.* (2007) The novel cargo Alcadein induces vesicle association of kinesin-1 motor components and activates axonal transport. *EMBO J.* **26**, 1475–1486.

Beel A. J., Mobley C. K., Kim H. J., Tian F., Hadziselimovic A., Jap B., Prestegard J. H. and Sanders C. R. (2008) Structural studies of the transmembrane C-terminal domain of the amyloid precursor protein (APP): does APP function as a cholesterol sensor? *Biochemistry* **47**, 9428–9446.

Buxbaum J. D., Liu K-N., Luo Y., Slack J. L., Stocking K. L., Peschon J. J., Johnson R. S., Castner B. J., Cerretti D. P. and Black R. A. (1998) Evidence that tumor necrosis factor αconverting enzyme is involved in regulated α-secretase cleavage of the Alzheimer amyloid protein precursor. *J. Biol. Chem.* **273**, 27765–27767.

Endes K., Postina R., Schoeder A., Mueller U. and Fahrenholz F. (2005) Shedding of the amyloid precursor protein-like protein APLP2 by disintegrin-metalloproteinases. *FEBS J.* **272**, 5808–5820.

Fang C., Deng L., Keller C. A., Fukata M., Fukata Y., Chen G. and Litscher B. (2006) GODZ-mediated palmitoylation of GABA(A) receptors is required for normal assembly and function of GABAergic inhibitory synapses. *J. Neurosci.* **26**, 12758–12768.

Fukata M., Fukata Y., Adesnik H., Nicoll R. A. and Bredt D. S. (2004) Identification of PSD-95 palmitoylating enzymes. *Neuron* **44**, 987–996.

Gandy S. (2005) The role of crebral amyloid β accumulation in common forms of Alzheimer disease. *J. Clin. Invest.* **115**, 1121–1129.

Gunawardena S. and Goldstein L. S. B. (2001) Disruption of axonal transport and neuronal viability by amyloid precursor protein mutations in *Drosophila*. *Neuron* **32**, 389–401.

Inomata H., Nakamura Y., Hayakawa A., Takata H., Suzuki T., Miyazawa K. and Kitamura N. (2003) A scaffold protein JIP-1b enhances amyloid precursor protein phosphorylation by JNK and its association with kinesin light chain 1. *J. Biol. Chem.* **278**, 22946–22955.

Lammich S., Kojro E., Postina R., Gilbert S., Pfeiffer R., Jasionoeski M., Haass C. and Fahrenholz F. (1999) Constitutive and regulated α-secretase cleavage of Alzheimer's amyloid precursor protein by a disintegrin metalloprotease. *Proc. Natl Acad. Sci. USA* **96**, 3922–3927.

Matsuda S., Yasukawa T., Homma Y. *et al.* (2001) c-Jun N-terminal kinae (JNK)-interacting protein-1b/islet brain-1 scaffolds Alzheimer's amyloid precursor protein with JNK. *J. Neurosci.* **21**, 6597–6607.

Mitchell D. A., Vasudevan A., Linder M. E. and Deschenes R. J. (2006) Protein palmitoylation by a family of DHHC protein S-acyltransferases. *J. Lipid Res.* **47**, 1118–1127.

Naruse S., Thinakaran G., Luo J. J. *et al.* (1998) Effects of PS1 deficiency on membrane protein trafficking in neurons. *Neuron* **21**, 1213–1221.

Offe K., Dodson S. E., Shoemaker J. T., Fritz J. J., Gearing M., Levey A. I. and Lah J. J. (2006) The lipoprotein receptor LR11 regulates amyloid β production and amyloid precursor protein traffic in endosomal compartments. *J. Neurosci.* **26**, 1596–1603.

Ohno Y., Kihara A., Sano T. and Igarashi Y. (2006) Intracellular localization and tissue-specific distribution of human and yeast DHHC cysteine-rich domain-containing proteins. *Biochim. Biophys. Acta* **1761**, 474–483.

Oishi M., Nairn A. C., Czernik A. J., Lim G. S., Isohara T., Gandy S. E., Greengard P. and Suzuki T. (1997) The cytoplasmic domain of Alzheimer's amyloid precursor protein is phosphorylated at Thr654, Ser655, and Thr668 in adult rat brain and cultured cells. *Mol. Med.* **3**, 111–123.

Roth A. F., Feng Y., Chen L. and Davis N. G. (2002) The yeast DHHC cysteine-rich domain protein Akr1p is a palmitoyltransferase. *J. Cell Biol.* **159**, 23–28.

Selkoe D. J. (2001) Alzheimer's disease: gene, proteins, and therapy. *Physiol. Rev.* **81**, 741–766.

Small S. A. and Gandy S. (2006) Sorting through the cell biology of Alzheimer's disease: intracellular pathways to pathogenesis. *Neuron* **52**, 15–31.

Stokin G. B., Lillo C., Falzone T. L. *et al.* (2005) Axonopathy and transport defects early in the pathogenesis of Alzheimer's disease. *Science* **307**, 1282–1288.

Suzuki T. and Nakaya T. (2008) Regulation of amyloid β-protein precursor by phosphorylation and protein interaction. *J. Biol. Chem.* **283**, 29633–29637.

Suzuki T., Araki Y., Yamamoto T. and Nakaya T. (2006) Trafficking of Alzheimer's disease-related membrane proteins and its participation in disease pathogenesis. *J. Biochem.* **139**, 949–955.

Taru H., Iijima K., Hase M., Kirino Y., Yagi Y. and Suzuki T. (2002) Interaction of Alzheimer's β-amyloid precursor family proteins with scaffold proteins of the JNK signaling cascade. *J. Biol. Chem.* **277**, 20070–20078.

Thinakaran G. and Koo E. D. (2008) Amyloid precursor protein trafficking, processing and function. *J. Biol. Chem.* **283**, 29615–29619.

Thomas G. (2002) Furin at the cutting rdge: from protein traffic to embryogenesis and disease. *Nat. Rev. Mol. Cell Biol.* **3**, 752–766.

Tomita S., Kirino Y. and Suzuki T. (1998) Cleavage of Alzheimer's amyloid precursor protein (APP) by secretase occurs after O-glycosylation of APP in the protein secretory pathway -Identification of intracellular compartments in which APP cleavage occurs without using toxic agents that interfere with protein metabolism. *J. Biol. Chem.* **273**, 6277–6284.

Wang H., Luo W. J., Zhang Y. W., Li M., Thinakaran G., Greengard P. and Xu H. (2004) Presenilins and gamma-secretase inhibitors affect intracellular trafficking and cell surface localization of the γ-secretase complex components. *J. Biol. Chem.* **279**, 40560–40566.

